

Electroweak Measurements from Hadron Machines

*Mark Lancaster
Department of Physics and Astronomy
University College London
London, WC1E 6BT, UK.*

1 Introduction

The discovery of the W and Z gauge bosons [1] at the $S\bar{p}\bar{p}S$ in 1983 marked the beginning of direct electroweak measurements at a hadron machine. These measurements vindicated the tree level predictions of the Standard Model. The new generation of hadron collider machines now have data of such precision that the electroweak measurements are probing the quantum corrections to the Standard Model. The importance of these quantum corrections was recognised in the award of the 1999 Nobel Prize [2]. These corrections are being tested by a wide variety of measurements ranging from atomic parity violation in caesium [3] to precision measurements at the Z pole [4] and above [5] in e^+e^- collisions. In this article, the latest experimental electroweak data from hadron machines is reviewed. I have taken a broad definition of a hadron machine to include the results from NuTeV [6] (νN collisions) and HERA [7, 8] (ep collisions) as well as the results from the Tevatron ($p\bar{p}$ collisions). This is not an exhaustive survey of all results [9], but a summary of the new results of the past year and in particular those results which have an influence on the indirect determination of the Higgs mass. This article will cover the direct determinations of the W boson and top quark masses from $p\bar{p}$ collisions at $\sqrt{s} = 1.8$ TeV from the two Tevatron experiments, CDF and DØ. These results are based on s -channel production of single W bosons and top quark pairs. The results presented here from the NuTeV and HERA experiments allow one to make complementary measurements and probe the electroweak interaction in the space-like domain up to large momentum transfers in the t -channel.

2 Data Samples

The first observation and measurements of the W boson were made at the CERN $S\bar{p}\bar{p}S$ by the UA1 and UA2 experiments. These measurements were based on modest event samples (~ 4 k events) and integrated luminosity (12 pb^{-1}). Since that time the Tevatron and LEP2 experiments have recorded over 1 fb^{-1} of W data. The Tevatron experiments have the largest sample of W events : over 180,000 from a combined integrated luminosity of $\sim 220 \text{ pb}^{-1}$. The LEP experiments, despite a very large integrated luminosity ($\sim 15000 \text{ pb}^{-1}$ total across all experiments), have event samples substantially smaller than the Tevatron experiments. The LEP2 W results [10] presented at this conference are based on event samples of ~ 6 k events per experiment. However, despite the smaller statistics of the W event sample in comparison to the Tevatron experiments, the LEP2 experiments ultimately achieve a comparable precision. On an event by event basis, the LEP2 events have more information; in particular the LEP2 experiments can impose energy and momentum constraints because they have a precise knowledge of the initial state through the beam energy measurement. The NuTeV experiment at FNAL has a large sample ($\sim 10^6$) of charged current events mediated by the t -channel exchange of a W boson. This allows an indirect determination of the W mass through a measurement of $\sin^2 \theta_w$. This is done by comparing the neutral and charged current cross

sections in νFe and $\bar{\nu}\text{Fe}$ collisions. The event samples available for electroweak tests at HERA are still rather modest and thus at present their results do not attain the precision of the $p\bar{p}$ and νN results. However, the ability to span a large range in momentum transfers and have both e^+p and e^-p collisions allows a number of unique electroweak observations to be made. The results from the Tevatron experiments on the top quark are now reaching their conclusion. These measurements based on only ~ 100 events selected from over 10^{12} $p\bar{p}$ collisions at the Tevatron represent what it is possible to achieve with a robust trigger and imaginative analysis techniques.

3 W Boson and Top Quark Mass Measurements

A precise W mass measurement allows a stringent test of the Standard Model beyond tree level where radiative corrections lead to a dependence of the W mass on both the top quark mass and the mass of the, as yet unobserved, Higgs boson. The dependence of the radiative corrections on the Higgs mass is only logarithmic whilst the dependence on the top mass is quadratic. Simultaneous measurements of the W and top masses can thus ultimately serve to further constrain the Higgs mass beyond the LEP1/SLD limits and potentially indicate the existence of particles beyond the Standard Model. Similarly, non Standard Model decays of the W would change the width of the W boson. A precise measurement of the W width can therefore be used to place constraints on physics beyond the Standard Model. The latest results on the W mass from the LEP2 and Tevatron experiments are now of such a precision that the uncertainty on the top mass is beginning to become the limiting factor in predicting the mass of the Higgs boson.

4 Latest Top Mass Measurements

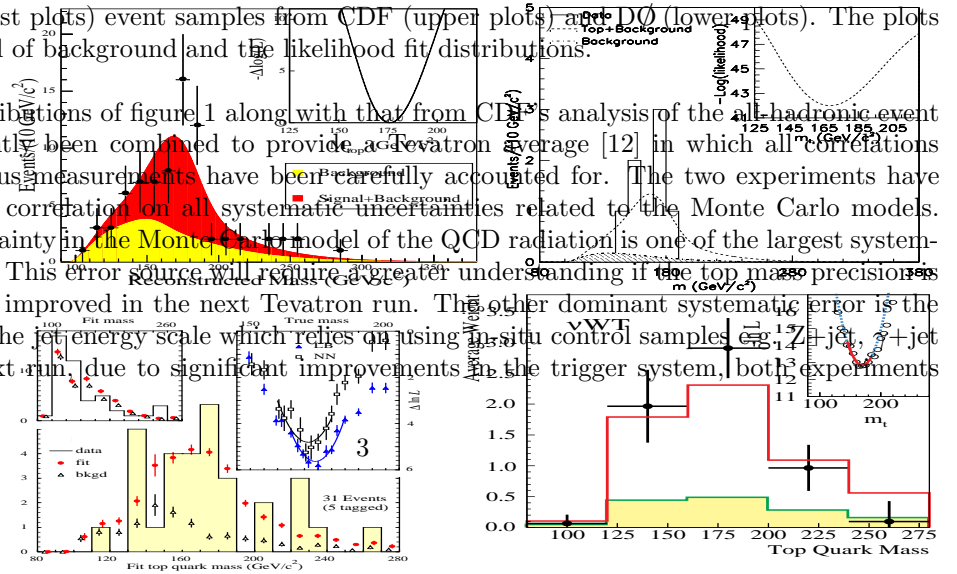
The top quark discovery at the Tevatron in 1995 was the culmination of a search lasting almost twenty years. The top quark is the only quark with a mass in the region of the electroweak gauge bosons and thus a detailed analysis of its properties could possibly lead to information on the mechanism of electroweak symmetry breaking. In particular, its mass is strongly affected by radiative corrections involving the Higgs boson. As such a measurement of the top mass with a precision < 10 GeV can provide information on the mass of the Higgs boson. The emphasis in top quark studies over the past two years at the Tevatron has thus been to make the most precise measurement of the top quark mass [11]. Substantial progress has been made in bringing the mass uncertainty down from > 10 GeV, at the point of discovery, to 5.1 GeV in 1999. In the past year, CDF has revised its systematic error analysis in the “all-hadronic” event sample and both experiments have published an analysis of the “di-lepton” event sample. The nomenclature of the event samples refers to the decay chain of the top quarks. At the Tevatron, top quarks are produced in pairs predominantly by $q\bar{q}$ annihilation and each top quark decays $> 99.9\%$ of the time to Wb . If both Ws decay to qq' , then the final state from the top system is $qq'qq'\bar{b}\bar{b}$ and the event sample is referred to as “all-hadronic”. Conversely, the “di-lepton” event sample is realised by selecting a $l^+\bar{\nu}l^-\nu\bar{b}\bar{b}$ final state, where both Ws have decayed leptonically (to e or μ). The “lepton+jet” event sample is one in which one W has decayed hadronically and one leptonically. The precision with which the top mass can be measured with each sample depends on the branching fractions, the level of background and how well constrained the system is. The all-hadronic sample has the largest cross section but has a large background from QCD six jet events ($S/N \sim 0.3$) whilst the di-lepton sample has a small background ($S/N \sim 4$) but suffers from a small cross section and the events are “under-constrained” since they contain two neutrinos. The optimum channel in terms of event sample size, background level and kinematic information content is the lepton+jet channel. Indeed this channel has a weight of $\sim 80\%$ in the combined Tevatron average. In the new “di-lepton” analysis, it is not possible to

perform a simple constrained fit for the top mass because the solution, owing to the two neutrinos, is under-constrained. One thus makes a comparison of the dynamics of the decay with Monte-Carlo expectations e.g. the \cancel{E}_T distribution and assigns an event weight to each possible solution of the fit : two for each top decay corresponding to the two-fold ambiguity in neutrino rapidity.

15240560780

Figure 1: The reconstructed top quark mass distributions in the lepton+jet (leftmost plots) and di-lepton (rightmost plots) event samples from CDF (upper plots) and DØ (lower plots). The plots also show the level of background and the likelihood fit distributions.

The mass distributions of figure 1 along with that from CDF's analysis of the all-hadronic event sample have recently been combined to provide a Tevatron average [12] in which all correlations between the various measurements have been carefully accounted for. The two experiments have assumed a 100 % correlation on all systematic uncertainties related to the Monte Carlo models. Indeed, the uncertainty in the Monte Carlo model of the QCD radiation is one of the largest systematic uncertainties. This error source will require a greater understanding if the top mass precision is to be significantly improved in the next Tevatron run. The other dominant systematic error is the determination of the jet energy scale which relies on using in-situ control samples e.g. Z+jet, γ +jet events. In the next run, due to significant improvements in the trigger system, both experiments



should be able to accumulate a reasonable sample of $Z \rightarrow b\bar{b}$ events which will be of great assistance in reducing the uncertainty in the b -jet energy scale.

The combined Tevatron mass value is 174.3 ± 3.2 (stat.) ± 4.0 (syst.) GeV. The individual mass measurements, the correlations between them and the relative weights of the measurements in the average are shown in figure 2.

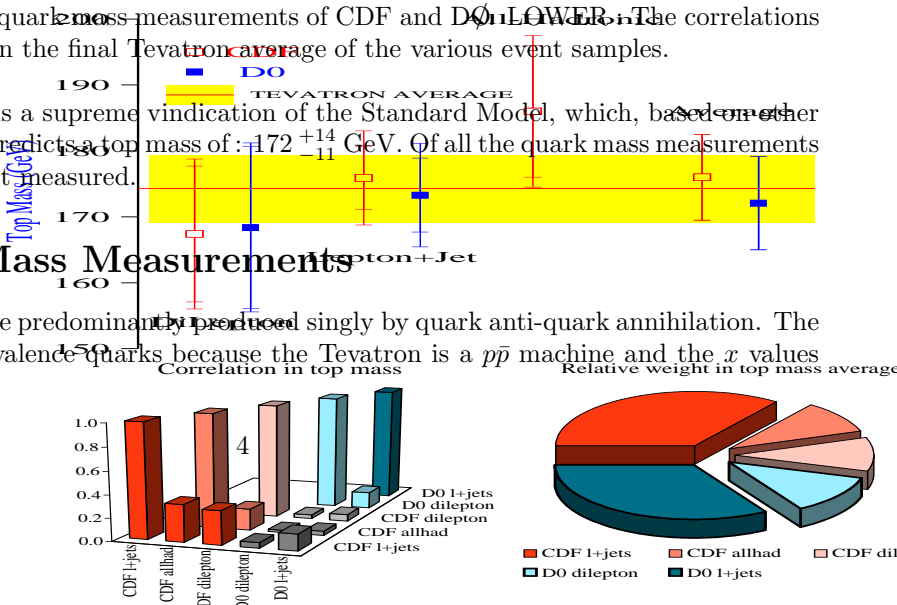
65220600850

Figure 2: UPPER : The top quark mass measurements of CDF and D0. LOWER : The correlations and weighted contributions in the final Tevatron average of the various event samples.

This mass measurement is a supreme vindication of the Standard Model, which, based on other electroweak measurements, predicts a top mass of 172^{+14}_{-11} GeV. Of all the quark mass measurements the top quark is now the best measured.

5 Tevatron W Mass Measurements

At the Tevatron W bosons are predominantly produced singly by quark anti-quark annihilation. The quarks involved are mostly valence quarks because the Tevatron is a $p\bar{p}$ machine and the x values



involved in W production ($0.01 \lesssim x \lesssim 0.1$) are relatively high. The W bosons are only detected in their decays to $e\nu$ (CDF and DØ) and $\mu\nu$ (CDF only) since the decay to qq' is swamped by the QCD dijet background whose cross section is over an order of magnitude higher in the mass range of interest. At the Tevatron one does not know the event \hat{s} and one cannot determine the longitudinal neutrino momentum since a significant fraction of the products from the $p\bar{p}$ interaction are emitted at large rapidity where there is no instrumentation. Consequently, one must determine the W mass from transverse quantities [13] namely : the transverse mass (M_T), the charged lepton P_T (P_T^l) or the missing transverse energy (\cancel{E}_T). \cancel{E}_T is inferred from a measurement of P_T^l and the remaining P_T in the detector, denoted by \vec{U} i.e.

$$\begin{aligned} \vec{\cancel{E}}_T &= -(\vec{U} + \vec{P}_T^l) & \text{and } M_T \text{ is defined as} \\ M_T &= \sqrt{2P_T^l \cancel{E}_T (1 - \cos \phi)} & \text{where } \phi \text{ is the angle between } \vec{\cancel{E}}_T \text{ and } \vec{P}_T^l \end{aligned}$$

\vec{U} receives contributions from two sources. Firstly, the so-called W recoil i.e. the particles arising from initial state QCD radiation from the $q\bar{q}$ legs producing the hard-scatter and secondly contributions from the spectator quarks ($p\bar{p}$ remnants) and additional minimum bias events which occur in the same crossing as the hard scatter. This second contribution is generally referred to as the underlying-event contribution. Experimentally these two contributions cannot be distinguished. Owing to the contribution from the underlying-event, the missing transverse energy resolution has a significant dependence on the instantaneous $p\bar{p}$ luminosity. M_T is to first order independent of the transverse momentum of the W (P_T^W) whereas P_T^l is linearly dependent on P_T^W . For this reason, and at the current luminosities where the effect of the \cancel{E}_T resolution is not too severe, the transverse mass is the preferred quantity to determine the W mass. However, the W masses determined from the P_T^l and \cancel{E}_T distributions provide important cross-checks on the integrity of the M_T result since the three measurements have different systematic uncertainties.

The systematics of the LEP2 and Tevatron measurements are very different and thus provide welcome complementary determinations of the W mass. The systematics at LEP2 are dominated by the uncertainty in the beam energy (which is used as a constraint in the mass fits) and by the modeling of the hadronic final state, particularly for the events where both W bosons decay hadronically. At the Tevatron, the systematics are dominated by the determination of the charged lepton energy scale and the Monte-Carlo modeling of the W production, in particular its P_T and rapidity distribution. At the Tevatron, one cannot use a beam energy constrain to reduce the sensitivity of the W mass to the absolute energy (E) and momentum (p) calibration of the detector. Any uncertainty in the detector E, p scales thus enters directly as an uncertainty in the Tevatron W mass. This means that the absolute energy and momentum calibration of the detectors must be known to better than 0.01%. By contrast at LEP, an absolute calibration of 0.5 % is sufficient.

The W mass at the Tevatron is determined through a precise simulation of the transverse mass line-shape, which exhibits a Jacobian edge at $M_T \sim M_W$. The simulation of the line-shape relies on a detailed understanding of the detector response and resolution to both the charged lepton and the recoil particles. This in turn requires a precise simulation of the W production and decay. The similarity in the production mechanism and mass of the W and Z bosons is exploited in the analysis to constrain many of the systematic uncertainties in the W mass analysis. The lepton momentum and energy scales are determined by a comparison of the measured Z mass from $Z \rightarrow e^+e^-$ and $Z \rightarrow \mu^+\mu^-$ decays with the value measured at LEP. The simulation of the W P_T and the detector response to it are determined by a measurement of the Z P_T which is determined precisely from the decay leptons and by a comparison of the leptonic (from the Z decay) and non-leptonic E_T quantities in Z events. The reliance on the Z data means that many of the systematic uncertainties in the W mass analyses are determined by the statistics of the Z sample.

The W and Z events in these analyses are selected by demanding a single isolated high P_T

charged lepton in conjunction with missing transverse energy (W events) or a second high P_T lepton (Z events). Depending on the analyses, the \cancel{E}_T cuts are either 25 or 30 GeV and the lepton P_T cuts are similarly 25 or 30 GeV. CDF only uses $W \rightarrow e\nu$ and $W \rightarrow \mu\nu$ events [14] in the rapidity region : $|\eta| < 1$, whereas DØ [15] uses $W \rightarrow e\nu$ events out to a rapidity of ~ 2.5 . In total $\sim 84k$ events are used in the W mass fits and $\sim 9k$ Z events are used for calibration.

5.1 Lepton Scale Determination

The lepton scales for the analyses are determined by comparing the measured Z masses with the LEP values. The mean lepton P_T in Z events ($P_T \sim 42$ GeV) is ~ 5 GeV higher than in W events, consequently in addition to setting the scale one also needs to determine the non-linearity in the scale determination i.e. to determine whether the scale has any P_T dependence. DØ does this by comparing the Z mass measured with high P_T electrons with J/ψ and π^0 masses measured using low P_T electrons as well as by measuring the Z mass in bins of lepton P_T . In the determination of CDF's momentum scale the non-linearity is constrained using the very large sample of $J/\psi \rightarrow \mu\mu$ and $\Upsilon \rightarrow \mu\mu$ events which span the P_T region : $2 < P_T < 10$ GeV. The non-linearity in the CDF transverse momentum scale is consistent with zero (see Fig. 3). This fact in turn can be exploited to determine the non-linearity in the electron transverse energy scale through a comparison of the measured E/p with a MC simulation of E/p where no E_T non-linearity is included. The lepton scale uncertainties form the largest contribution to the W mass systematic error. The non-linearity contribution to the scale uncertainty is typically $\sim 10\%$ or less.

The Z lineshape is also used by both experiments to determine the charged lepton resolution functions i.e. the non-stochastic contribution to the calorimeter resolution and the curvature tracking resolution in the case of the CDF muon analysis.

5.2 W Production Model

The lepton P_T and \cancel{E}_T distributions are boosted by the non zero P_T^W and the \cancel{E}_T vector is determined in part from the W-recoil products. As such a detailed simulation of the P_T^W spectrum and the detector response and resolution functions is a necessary ingredient in the W mass analysis. The W P_T distribution is determined by a measurement of the Z P_T distribution (measured from the decay leptons) and a theoretical prediction of the W to Z P_T ratio. This ratio is known with a small uncertainty and thus the determination of the W P_T is dominated by the uncertainty arising from the limited size of the Z data sample. The P_T^Z distribution of the CDF $Z \rightarrow \mu^+\mu^-$ sample is shown in Fig. 3. The detector response and resolution functions to the W-recoil and underlying event products are determined by both experiments using Z and minimum bias events. Since the W-recoil products are typically produced along the direction of the vector boson P_T and the underlying event products are produced uniformly in azimuth, the response and resolution functions are determined separately in two projections – one in the plane of the vector boson and one perpendicular to it. Typically one finds the resolution in the plane of the vector boson is poorer owing to the presence of jets (initial state QCD radiation from the quark legs) which are absent in the perpendicular plane where the resolution function matches closely that expected from pure minimum bias events. The parton distribution functions (PDFs) determine the rapidity distribution of the W and hence of the charged lepton. Both experiments impose cuts on the rapidity of the charged lepton and so a reliable simulation of this cut is necessary if the W mass determination is not to be biased. On average the u quark is found to carry more momentum than the d quark resulting in a charge asymmetry of the produced W i.e. $W^{+(-)}$ are produced preferentially along the $(p\bar{p})$ direction. Since the V-A structure of the W decay is well understood, a measurement of the charged lepton asymmetry therefore serves as a reliable means to constrain the PDFs. To determine the uncertainty in the W mass arising from

20190565485

Figure 3: LEFT: The CDF determination of the momentum scale and non-linearity using dimuon resonances. RIGHT UPPER: The modified PDF sets used in the Mw analysis, which span CDF's W charge asymmetry measurement. RIGHT LOWER : The Z P_T distribution as measured by CDF in the $Z \rightarrow \mu^+\mu^-$ channel.

PDFs, MRS PDFs were modified to span the CDF charged lepton asymmetry measurements [16]. This is illustrated in Fig. 3.

5.3 Mass Fits

The W mass is obtained from a maximum likelihood fit of M_T templates generated at discrete values of M_W with Γ_W fixed at the Standard Model value. The templates also include the background distributions, which are small ($< 5\%$) and have three components : $W \rightarrow \tau\nu$, followed by $\tau \rightarrow \mu/\nu\nu$, QCD processes where one mis-measured jet mimics the \cancel{E}_T signature and the other jet satisfies the charged lepton identification criteria and finally Z events where one of the lepton legs is not detected. The transverse mass fits for the $D\phi$ end-cap electrons and the two CDF measurements are shown in Fig. 4. The uncertainties associated with the measurements are listed in Table 1. The uncertainties of the published $D\phi$ central-electron analysis are also listed. For both experiments the largest errors are statistical in nature, both from the statistics of the W sample and also the statistics of the Z samples which are used to define many of the systematic uncertainties e.g. the uncertainties in the lepton energy/momentum scales and the W P_T model. The CDF and $D\phi$ measurements are combined with a 25 MeV common uncertainty which accounts for the uncertainties in PDFs and QED radiative corrections which by virtue of being constrained from the same source are highly correlated. Together the two experiments yield a W mass value of 80.450 GeV with an uncertainty of 63 MeV. For the first time, both Tevatron experiments have measurements with uncertainties below 100 MeV and the combined uncertainty is comparable with the LEP2 results presented at this conference.

40100530430

Figure 4: Transverse mass distributions compared to the best fit. LEFT : DØ’s published central-electron analysis and preliminary end-cap analysis. RIGHT : CDF’s electron and muon channel analyses. The fit likelihood and residuals are also shown for the two DØ distributions.

6 W Mass Result from NuTeV

Neutrino scattering experiments have contributed to our understanding of electroweak physics for more than three decades. Early determinations of $\sin^2 \theta_W$ served as the critical ingredient to the Standard Model’s successful prediction of the W and Z boson masses. More precise investigations in the late 1980’s set the first useful limits on the top quark mass. The recent NUTEV measurement of the electroweak mixing angle from neutrino-nucleon scattering represents the most precise determination to date. The result is a factor of two more precise than the previous most accurate νN measurement [17]. In deep inelastic neutrino-nucleon scattering, the weak mixing angle can be extracted from the ratio of neutral current (NC) to charged current (CC) total cross sections. Previous measurements relied on the Hewell-Smith formula, which relates these ratios to $\sin^2 \theta_W$ for neutrino scattering on isoscalar targets [18]. However such measurements were plagued by large uncertainties in the charm contribution (principally due to the imprecise knowledge of the charm quark mass). An alternate method for determining $\sin^2 \theta_W$ that is much less dependent on the details of charm production and other sources of model uncertainty is derived from the Paschos-Wolfenstein quantity, R^- [19] :

Error Source	DØ (EC)	DØ (C)	CDF (e)	CDF (μ)
Statistical	70	105	65	100
Lepton Scale+Resolution	70	185	80	90
$P_T^W + E_T$ Model	35	50	40	40
Other experimental	40	60	5	30
Theory (PDFs, QED)	30	40	25	20
Total Error	120	235	113	143
Mass Value	80.440	80.766	80.473	80.465
Combined Mass Values	80.497 ± 0.098 GeV		80.470 ± 0.089 GeV	

Table 1: The mass values and uncertainties of the CDF and DØ W mass analyses using the 1994–1995 data. The uncertainties are quoted in MeV. The mass values when the 1992–1993 data are included become : 80.474 ± 0.093 GeV for DØ and 80.430 ± 0.079 GeV for CDF. (EC) denotes the large rapidity end-cap analysis and (C) denotes the central rapidity analysis.

$$R^- \equiv \frac{\sigma(\nu_\mu N \rightarrow \nu_\mu X) - \sigma(\bar{\nu}_\mu N \rightarrow \bar{\nu}_\mu X)}{\sigma(\nu_\mu N \rightarrow \mu^- X) - \sigma(\bar{\nu}_\mu N \rightarrow \mu^+ X)} = \frac{R^\nu - rR^{\bar{\nu}}}{1 - r} = \frac{1}{2} - \sin^2 \theta_W \quad (1)$$

Because R^- is formed from the difference of neutrino and anti-neutrino cross sections, almost all sensitivity to the effects of sea quark scattering cancels. This reduces the error associated with heavy quark production by roughly a factor of eight relative to the previous analysis. The substantially reduced uncertainties, however, come at a price. The ratio R^- is difficult to measure experimentally because neutral-current neutrino and anti-neutrino events have identical observed final states. The two samples can only be separated via *a priori* knowledge of the incoming neutrino beam type. This is done by using the FNAL Sign Selected Quadrupole Train (SSQT) which selects mesons of the appropriate sign. The measured $\bar{\nu}_\mu$ contamination in the ν_μ beam is less than 1/1000 and the ν_μ contamination in the $\bar{\nu}_\mu$ beam is less than 1/500. In addition, the beam is almost purely muon-neutrino with a small contamination of electron neutrinos (1.3% in neutrino mode and 1.1% in anti-neutrino mode). The NC and CC events are selected by their characteristic event length : the CC events produce a muon and thus register activity in the detector over a long length, whereas NC events just produce a short hadronic shower. This is illustrated in figure 5 where the two event-length contributions to the event sample are shown. The events are separated by a cut at the 20th counter i.e. after ~ 2 m of steel.

From the νN interactions, 386 *k* NC and 919 *k* CC events are recorded and from the $\bar{\nu} N$ sample 89 *k* NC and 210 *k* CC events. The extracted value of $\sin^2 \theta_W(\text{on-shell}) = 0.2254 \pm 0.0021$ which can be translated into an Mw value of 80.26 ± 0.1 (stat.) ± 0.05 (syst.) GeV, where the systematic error also receives a contribution from the unknown Higgs mass.

7 Electroweak Results from HERA

The two HERA experiments, ZEUS and H1, are now beginning to probe the electroweak interaction in the space-like domain at scales of $\sim 10^{-3}$ fm. The results up to Q^2 values of 40,000 GeV² are in good agreement with the Standard Model predictions. The use of both e^+p and e^-p collisions and the fact that the experiments can measure both neutral current and charged current processes, allows one to directly observe electroweak unification in a single experiment. This is illustrated in figure 6 where both the neutral current and charged current cross sections are shown as a function

00580290

Event Length (counters, 10cm Steel)

Figure 5: The event length distributions (dark : NC events, light : CC events) as a function of the number of counters for the ν and $\bar{\nu}$ beams. The level of ν_e contamination is also shown.

of the Q^2 . At low Q^2 , the neutral current cross section, mediated by γ exchange, dominates; but as Q^2 increases one observes the emergence of the charged current cross section (mediated by W exchange) with a magnitude comparable to that of the neutral current cross section (which becomes dominated by Z_0 exchange at high Q^2). The detailed comparison of the four cross sections can be used to measure parton distributions : in particular one can separate the light quark contributions to the cross sections and determine the u and d quark distributions [20]. By using the helicity variable y , where y is related to the scattering angle in the electron-quark center of mass frame, via : $(1 - y) = \cos^2 \frac{\theta}{2}$ and measuring the γ -CC cross section as a function of $(1 - y)^2$ one observes direct evidence for the $\gamma - Z_0$ interference contribution to the NC cross section at high Q^2 .

Although the HERA experiments have only produced a handful of direct W s, they have several thousand charged current events in which a virtual W is exchanged in the t -channel. From a measurement of the Q^2 dependence of the cross section one becomes sensitive to the charged current propagator and hence W mass. This determination (see figure 7) of the W mass agrees with the direct determinations but is presently uncompetitive owing to the statistical uncertainty and the systematics associated with parton distribution functions : an uncertainty which can also be reduced with more data. This determination is made more powerful if one also considers the magnitude of the charged current cross section and assumes the Standard Model relation between G_F and M_W and M_Z . This relation also receives radiative corrections which depend on the masses of the fundamental gauge bosons and fermions. One thus has a dependence on M_W in both the Q^2 variation (propagator) and the cross section magnitude (via G_F). By fixing the measured cross section to the Standard Model value, one can obtain a W mass value with an uncertainty of ~ 400 MeV.

29164541668

Figure 6: The NC and CC e^+p and e^-p cross sections from ZEUS as a function of Q^2 .

8 Comparison of Mw results

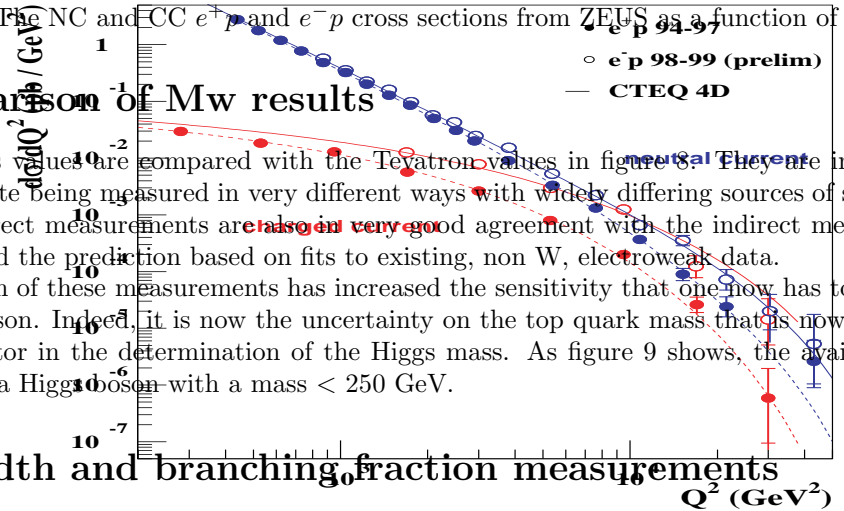
The LEP2 mass values are compared with the Tevatron values in figure 8. They are in excellent agreement despite being measured in very different ways with widely differing sources of systematic error. These direct measurements are also in very good agreement with the indirect measurement from NuTeV and the prediction based on fits to existing, non W, electroweak data.

The precision of these measurements has increased the sensitivity that one now has to the mass of the Higgs Boson. Indeed, it is now the uncertainty on the top quark mass that is now becoming the limiting factor in the determination of the Higgs mass. As figure 9 shows, the available data tends to favour a Higgs boson with a mass < 250 GeV.

9 W Width and branching fraction measurements

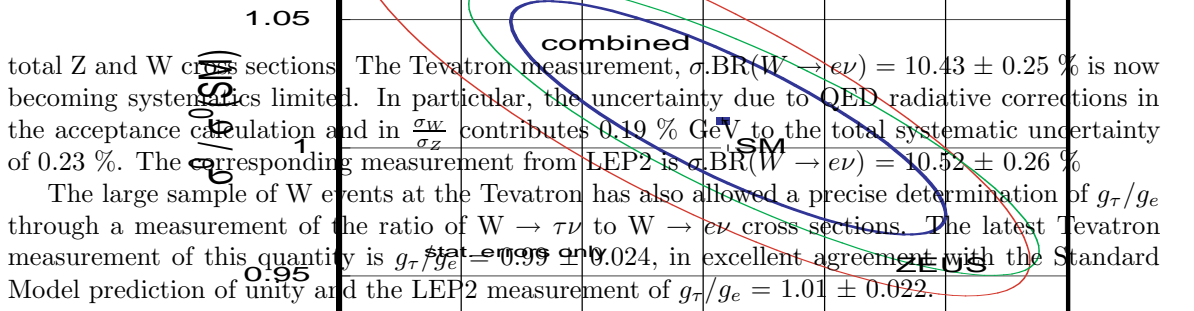
The Tevatron presently has the most precise direct determination of the W width and has measurements of the W branching fractions comparable in precision to the LEP2 measurements. The Tevatron experiments determine the width by a one parameter likelihood fit to the high transverse mass end of the transverse mass distribution. Detector resolution effects fall off in a Gaussian manner such that at high transverse masses ($M_T \gtrsim 120$ GeV), the distribution is dominated by the Breit-Wigner behaviour of the cross section (see figure 10). In the fit region, CDF has 750 events, in the electron and muon channels combined.

At LEP2, the W branching fractions are determined by an explicit cross section measurement whilst at the Tevatron they are determined from a measurement of a cross section ratio. Specifically, the W branching fraction can be written as : $\sigma \cdot \text{BR}(W \rightarrow e\nu) = \frac{\sigma_W}{\sigma_Z} \cdot \frac{\Gamma(Z \rightarrow ee)}{\Gamma(Z)}$; where $R = \frac{\sigma_W \cdot \text{BR}(W \rightarrow e\nu)}{\sigma_Z \cdot \text{BR}(Z \rightarrow ee)}$ is the measurement made at the Tevatron. This determination thus relies on the LEP1 measurement of the Z branching fractions and the theoretical calculation of the ratio of the



22110520690

Figure 7: The HERA charged current cross section compared to the SM prediction as a function of the propagator mass, M_W .

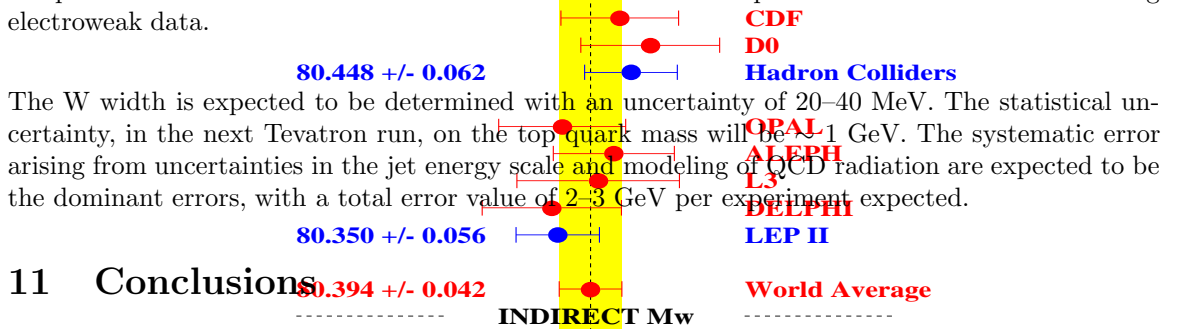


10 Outlook

The majority of electroweak results presented here are presently dominated by statistical uncertainties : either directly or in the control/calibration samples. For NuTeV no further data is planned and thus the precision of their measurement of $\sin^2 \theta_W$ will remain dominated by the statistical uncertainty. In contrast, both the Tevatron and HERA are undergoing luminosity upgrades augmented with substantial improvements in the collider's detectors. At HERA, 150pb^{-1} per year per experiment is expected, as is the availability of polarised electrons and positrons in ep collider mode. At the Tevatron, at least 2fb^{-1} is expected per experiment at an increased center of mass energy of 2 TeV. It is expected that both the top quark mass and W mass measurements will become limited by systematic uncertainties. The statistical part of the Tevatron W mass error in the next run will be ~ 10 MeV, where this also includes the part of the systematic error which is statistical in nature e.g. the determination of the charged lepton E and p scales from Z events. At present the errors non-statistical in nature contribute 25 MeV out of the total Tevatron W mass error of 60 MeV. A combined W mass which is better than the final LEP2 uncertainty can thus be anticipated [21].

1515530430

Figure 8: The direct determinations of the W mass from the Tevatron and LEP2 experiments are compared with the indirect measurement from NuTeV and the prediction based on fits to existing electroweak data.



11 Conclusions

The hadron collider experiments continue to make significant contributions to electroweak physics which complement those from e^+e^- machines. The higher cross sections and \sqrt{s} allow some unique measurements to be made e.g. the mass of the top quark. The precision of many measurements is comparable to, if not better than, that achieved by e^+e^- machines. All results : top mass, W mass, W width, branching fractions, $\sin^2 \theta_W$, cross sections etc are in excellent agreement with the Standard Model in a range of processes : $qq, eq, \nu q$ over a wide span in Q^2 . The future is bright and significant new results are expected from the Tevatron and HERA experiments before the LHC.

References

- [1] G. Arnison *et al.*, Phys. Lett. **B122** 103 (1983), M. Banner *et al.*, Phys. Lett. **B122** 476 (1983), C. Albajar *et al.*, Z. Phys. **C44** 15 (1989), J. Aliti *et al.*, Phys. Lett. **B277** 354 (1992).
- [2] <http://www.nobel.se/announcement-99/physics99.html>
- [3] C.S. Wood *et al.*, Science **275**, 1759 (1997).

30180560650

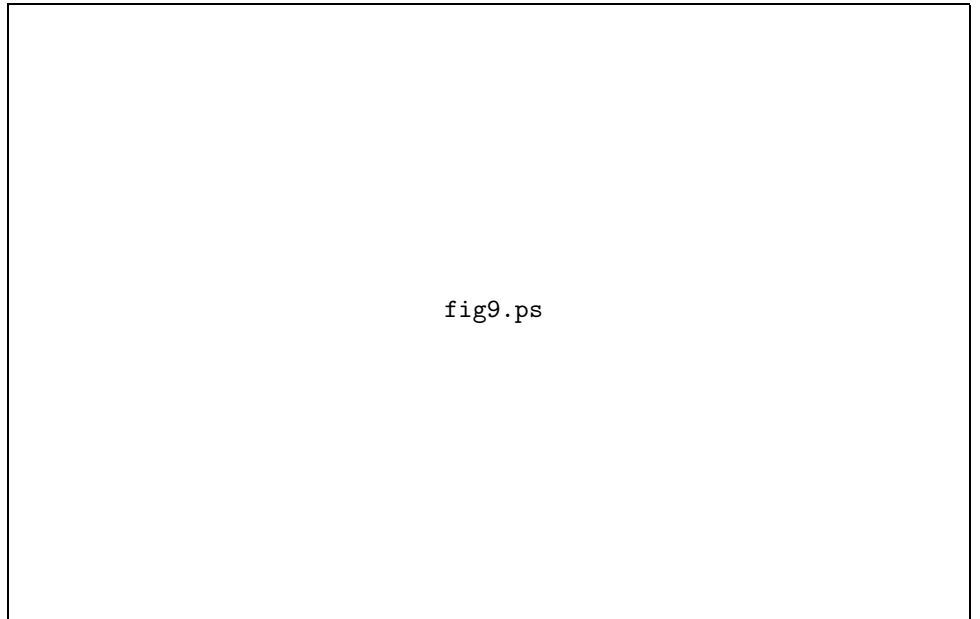
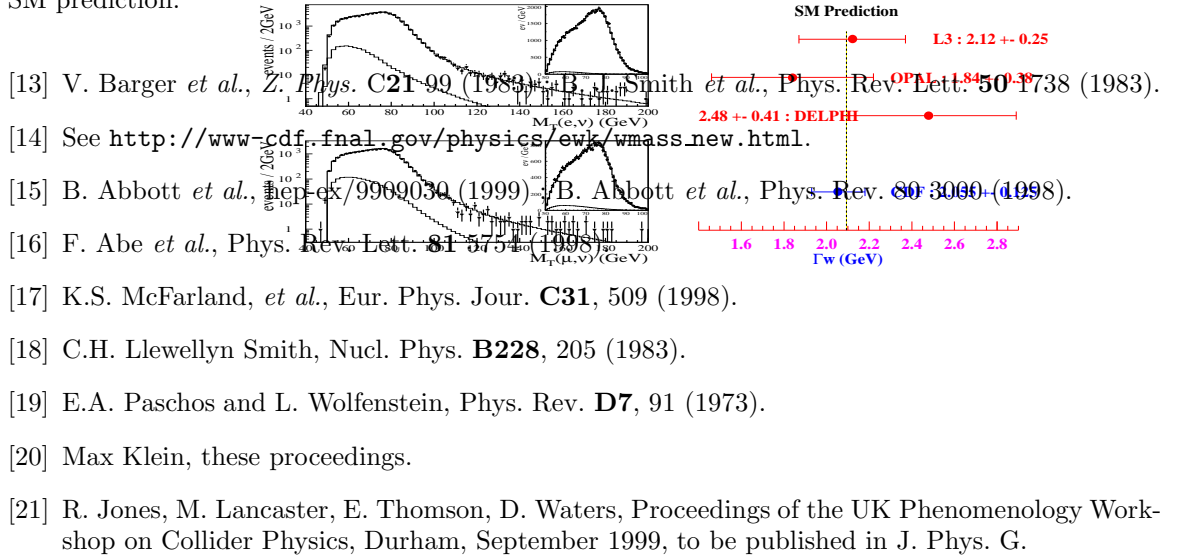


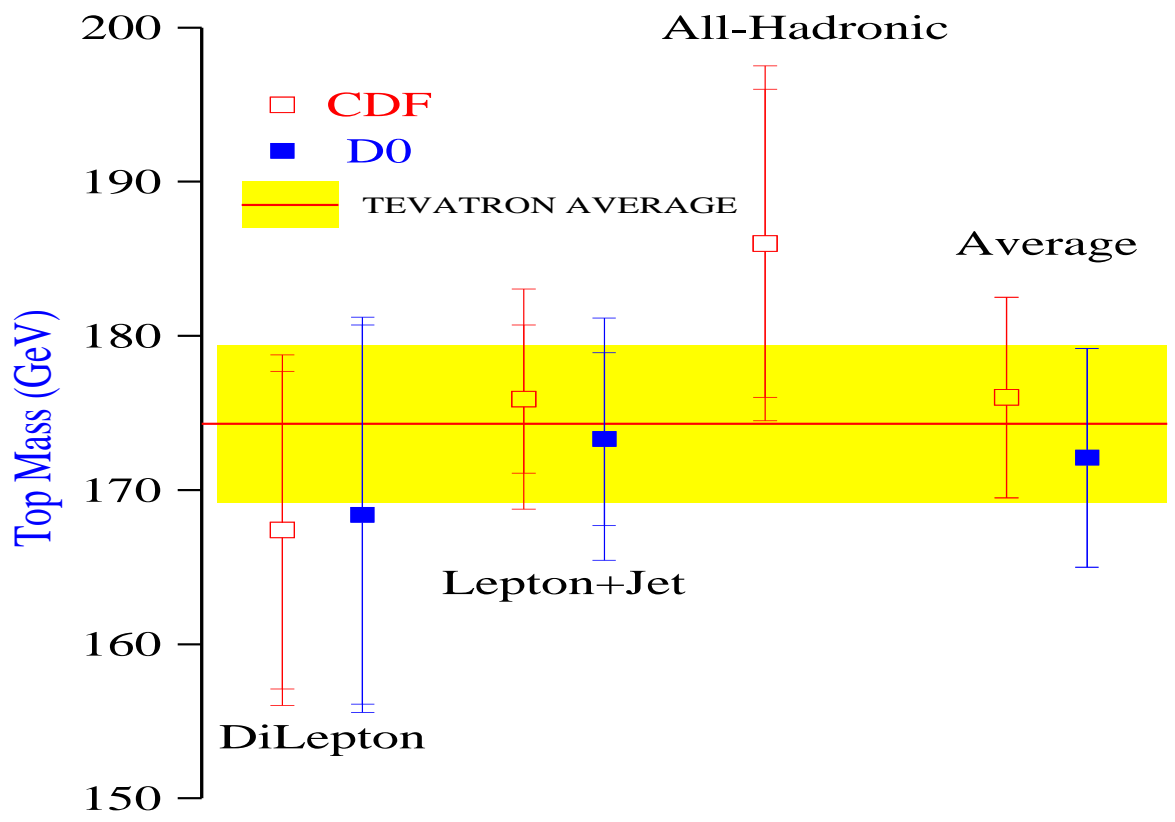
Figure 9: The direct measurements of the W boson and top quark mass from the Tevatron experiments are compared to the W mass measurements from LEP2 and the predictions based on electroweak fits to LEP1/SLD/ ν N data. The Standard Model predictions for the Higgs mass as a function of the W and top masses are also shown.

- [4] Morris Swartz, these proceedings.
- [5] David Charlton, these proceedings.
- [6] NuTeV Collaboration, hep-ex/9906024.
- [7] C. Adloff *et al.*, DESY-99-107 and abstracts 157s, 157ai, 157b submitted to the International Europhysics Conference on High Energy Physics, Tampere, Finland, July 1999.
- [8] J. Breitweg *et al.*, DESY-99-054,056,059 and abstracts 549, 550, 558, 559 submitted to the International Europhysics Conference on High Energy Physics, Tampere, Finland, July 1999.
- [9] See <http://www.pdg.gov/1999/stanmodelrpp.pdf> and references therein.
- [10] K. Ackerstaff *et al.*, Phys. Lett. **B389** 416 (1996); R. Barate *et al.*, Phys. Lett. **B401** 347 (1997); M. Acciarri *et al.*, Phys. Lett. **B398** 223 (1997); P. Abreu *et al.*, Phys. Lett. **B397** 158 (1997); ALEPH Collaboration, CERN-EP/99-027; DELPHI Collaboration, DELPHI 99-41 CONF 240; L3 Collaboration, CERN-EP/99-17; OPAL Collaboration, CERN-EP/98-197; ALEPH Collaboration, ALPEH 99-015 CONF 99-010; ALEPH Collaboration, ALPEH 99-017 CONF 99-012; DELPHI Collaboration, DELPHI 99-51 CONF 244; L3 Collaboration, L3 Note 2377; OPAL Collaboration, Physics Note PN385.
- [11] F. Abe *et al.*, Phys. Rev. Lett. **82** 271 (1999); S. Abachi *et al.*, *Phys. Rev. D* **58** 052001 (1998).
- [12] L. Demortier *et al.*, FNAL-TM-2084 (1999).

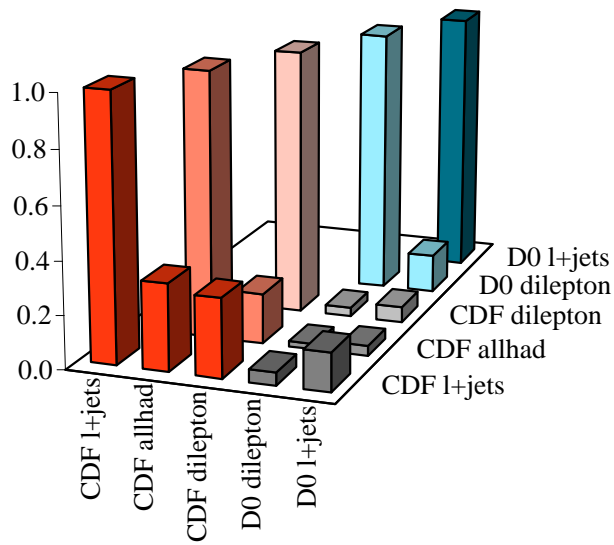
30220570640

Figure 10: LEFT: The transverse mass distribution of the CDF $W \rightarrow e\nu$ (upper) and $W \rightarrow \mu\nu$ (lower) data showing the events at high transverse mass from which the W width is determined. RIGHT: A comparison of the direct W width determinations from LEP and the Tevatron with the SM prediction.





Correlation in top mass



Relative weight in top mass average

